Bio-inspired pulmonary surfactant-modified nanogels: a promising siRNA delivery system.

Authors
Lynn De Backer[a], Kevin Braeckmans[a], Marc C.A. Stuart[b], Jo Demeester[a], Stefaan C. De Smedt[a,]*, and Koen Raemdonck[a].

Affiliation
[a] Laboratory of General Biochemistry and Physical Pharmacy, Faculty of Pharmacy, Ghent University. Ottergemsesteenweg 460, 9000 Ghent, Belgium.
[b] Department of Electron Microscopy, Groningen Biomolecular Sciences and Biotechnology Institute, University of Groningen. Nijenborgh 7, 9747 AG Groningen, The Netherlands.

*** Corresponding author:**
Stefaan C. De Smedt. Tel.: +3292648076; Fax: +3292648189

E-mail addresses authors
lynn.debacker@ugent.be; kevin.braeckmans@ugent.be; m.c.a.stuart@rug.nl; jo.demeester@ugent.be; stefaan.desmedt@ugent.be; koen.raemdonck@ugent.be

Abstract
Inhalation therapy with small interfering RNA (siRNA) is a promising approach in the treatment of pulmonary disorders. However, clinical translation is severely limited by the lack of suitable delivery platforms. In this study, we aim to address this limitation by designing a novel bioinspired hybrid nanoparticle with a core-shell nanoarchitecture, consisting of a siRNA-loaded dextran nanogel (siNG) core and a pulmonary surfactant (Curosurf®) outer shell. The decoration of siNGs with a surfactant shell enhances the colloidal stability and prevents siRNA release in the presence of competing polyanions, which are abundantly present in biofluids. Additionally, the impact of the surfactant shell on the biological efficacy of the siNGs is determined in lung cancer cells. The presence of the surfactants substantially reduces the cellular uptake of siNGs. Remarkably, the lowered intracellular dose does not impede the gene silencing effect, suggesting a crucial role of the pulmonary surfactant in the intracellular processing of the nanoparticles. In order to surmount the observed reduction in cellular dose, folate is incorporated as a targeting ligand in the pulmonary surfactant shell to incite receptor-mediated endocytosis. The latter substantially enhances both cellular uptake and gene silencing potential, achieving efficient knockdown at siRNA concentrations in the low nanomolar range.

1. Introduction

RNA interference (RNAi) represents a powerful process that regulates gene expression in eukaryotic cells on the post-transcriptional level. Sequence-specific cleavage of mRNA transcripts *via* RNAi can be initiated by synthetic RNA duplexes, termed small interfering RNA (siRNA). Since siRNAs can be designed to repress the expression of any gene of interest, they are being extensively investigated for the treatment of various diseases by blocking the expression of disease-related proteins [1-3]. More than 20 clinical trials have already been conducted involving siRNA-mediated therapy. However, despite intensive research efforts, to date no RNAi-based therapeutic has advanced into the clinic [4, 5].
One of the major bottlenecks impeding its clinical translation is the lack of biocompatible siRNA carriers that can overcome the various extra- and intracellular barriers to deliver the

siRNA to the target cell cytoplasm [6, 7]. To date, the most widely studied siRNA delivery systems include polymer-[8, 9] and lipid-based [10-12] nanoparticles. Earlier work from our group demonstrated the feasibility of cationic dextran nanosized hydrogels (nanogels) for siRNA delivery. These nanogels (NGs) encompass a high loading capacity for siRNA (exceeding 50 wt%), are efficiently internalized by cultured cells and are able to induce a marked RNAi effect *in vitro* [13].

Unfortunately, polymer- or lipid-based siRNA-loaded nanoparticles often fail to surmount the numerous biological barriers en route to their intracellular target *in vivo*. In order to address the multifaceted drug delivery challenges, several research groups aim to combine the unique strengths of both polymers and lipids within a single delivery vehicle, to obtain lipid-polymer nanocomposites [14-16]. Hybrid lipid-polymer nanoparticles have emerged as a robust and promising delivery platform for *in vivo* siRNA delivery upon systemic administration [17, 18]. However, their potential in local pulmonary applications remains largely unexplored, while respiratory diseases constitute a global health problem and inhalation therapy with siRNA nanomedicines could address the unmet therapeutic need for various pulmonary disorders [19-21].

Apart from the hybrid lipid-polymer nanoparticles, there is a growing interest as well in the implementation of *bio-inspired* materials in drug delivery vehicles. These materials are believed to possess specific features from which drug carriers could benefit, including an improved *in vivo* stability, biocompatibility, and intrinsic cell-targeting [22, 23]. In terms of drug delivery to the lung, the value of pulmonary surfactants as a drug carrier as such, or in combination with other nanomedicines, has been suggested [24-28]. In a recent study from our group, natural-derived pulmonary surfactants (e.g. Curosurf®) were used as a model to assess the impact that pulmonary surfactant might have on the delivery potential of siRNA-loaded NGs (siNGs) [29]. Surprisingly, these data already revealed that pulmonary surfactants play a crucial unknown role in the cellular processing of the siNGs in lung-specific cell types, resulting in an improved cytosolic delivery of the encapsulated siRNA. However, the approach to combine the beneficial features of both siNGs and pulmonary surfactant in a *single delivery vehicle* has not yet been evaluated. Moreover, the inclusion of a targeting moiety to further boost the delivery process has not been attempted to date. Therefore, the major aim of this work is to design a core-shell formulation consisting of siNGs endowed with a clinically approved pulmonary surfactant (Curosurf®) shell. Both the colloidal stability and the siRNA release profiles in the presence of competing polyanions, i.e. mucin and dextran sulfate, are evaluated. The core-shell nanoarchitecture is assessed *via* cryo-TEM imaging. Furthermore, it is investigated if the presence of the surfactant coat could enhance the biological efficacy of the siNGs, and if it could be employed for anchoring a targeting moiety to stimulate cellular uptake and further enhance siRNA delivery in lung cancer cells. Finally, the intracellular fate of the different nanoparticles is evaluated *via* confocal fluorescence microscopy and colocalization analysis.

2. Materials and methods

2.1. siRNA duplexes

Twenty-one nucleotide siRNA duplexes targeted against Enhanced Green Fluorescent Protein (EGFP), hereafter abbreviated as siEGFP, and non-targeting negative control duplexes (siCTRL) were purchased from Eurogentec (Seraing, Belgium). SiEGFP: sense strand = 5′-CAAGCUGACCCUGAAGUUCtt-3′; antisense strand = 5′-GAACUUCAGGGUCAGCUUG tt-3′. SiCTRL: sense strand = 5′-UGCGCUACGAUCGACGAUGtt-3′; antisense strand = 5′-CAUCGUCGAUCGUAGCGCAtt-3′ (capital letters represent ribonucleotides; lower case letters represent 2′-deoxyribonucleotides). For fluorescence experiments, the siCTRL duplex

was labeled with a Cy5 dye at the 5' end of the sense strand (siCy5). The fluorescent modifications were performed and verified by Eurogentec. The concentration of the siRNA stock solutions in nuclease free water (Ambion®-Life Technologies, Ghent, Belgium) was calculated from absorption measurements at 260 nm (1 OD_{260} = 40 µg mL^{-1}) with a Nanodrop 2000 spectrophotometer (Thermo Fisher Scientific, DE, USA).

2.2. Synthesis of dextran nanogels and loading with siRNA

Cationic dextran nanogels were prepared using an inverse mini-emulsion photopolymerization method as reported previously [13]. Briefly, 65 mg of dextran hydroxyethyl methacrylate (dex-HEMA; degree of substitution 5.2) [30] was dissolved in a solution containing 40 µL irgacure 2959 (10 mg mL^{-1} in water; Sigma-Aldrich, Bornem, Belgium), 80 µL nuclease free water and 40 µL of a cationic methacrylate monomer, [2-(methacryloyloxy)-ethyl] trimethylammonium chloride (TMAEMA, 80 wt% solution in water; Sigma-Aldrich). The obtained dex-HEMA solution was emulsified in 5 mL of mineral oil (Sigma-Aldrich), supplemented with 10 % (v/v) of the surfactant ABIL EM 90 (Evonik Goldschmidt GmbH, Essen, Germany), through ultrasonication (50 s, amplitude 15 %; Branson Digital Sonifier®, CT, USA). The formed emulsion nanodroplets were immediately crosslinked by UV irradiation (900 s, Bluepoint 2.1 UV source, Hönle UV technology, Gräfelfing, Germany) under cooling (4°C). The resulting dex-HEMA-*co*-TMAEMA nanogels, hereafter abbreviated as NGs, were collected by precipitation in acetone, and washed three times with acetone:hexane (1:1). Traces of organic solvent were removed by vacuum evaporation and the pellet was redispersed in 5 mL nuclease free water. To assure long-term stability, the NGs were lyophilized and stored desiccated.

To obtain siRNA-loaded NGs (siNGs), first a NG stock (2 mg mL^{-1}) was prepared by dispersing a weighed amount of lyophilized particles in ice-cooled nuclease free water, followed by brief sonication (amplitude 10 %). Subsequently, equal volumes of NG and siRNA dilutions in N-2-hydroxyethylpiperazine-N'-2-ethanesulfonic acid (HEPES) buffer (pH 7.4, 20 mM) were mixed and incubated at 4 °C for ≥ 15 min to allow complexation.

2.3. Preparation of pulmonary surfactant-coated nanogels

A commercially available pulmonary surfactant, derived from minced porcine lungs (Curosurf®; Chiesi Pharmaceuticals, Parma, Italy), was used to construct the pulmonary surfactant shell. For a detailed discussion on the different lipid and protein constituents, the reader is referred to recent articles on this topic [31, 32]. Prior to the formation of the pulmonary surfactant coat, the NGs were loaded with siRNA, as described above. For the second step, where the siNGs interact with the pulmonary surfactant, two different protocols were evaluated. In the first protocol, Curosurf® (diluted in HEPES buffer) was homogenized using a probe sonicator to form surfactant vesicles prior to mixing with the siNGs. The hybrid nanoparticles obtained *via* this approach are further abbreviated as *coated siNGs-1*. In the alternate protocol, the unprocessed Curosurf® dispersion was first incubated with siNGs for 10 min at 4 °C, after which the surfactant coat was formed by high-energy sonication, using a probe sonicator (amplitude 10 %). This resulted in a hybrid nanoparticle further denoted as *coated siNGs*-2. Depending on the experimental needs, different surfactant-to-NG weight ratios were used.

To evaluate the influence of salt during the preparation of the coated siNGs-2 formulation, siRNA and NGs were diluted in phosphate buffered saline (PBS; Invitrogen, Merelbeke, Belgium). PBS has a 15-fold higher osmolality (280-315 mOsm kg^{-1}) compared to HEPES buffer (20 mOsm kg^{-1}). After 15 min incubation (4 °C), Curosurf® (diluted in PBS) was added to the siNGs and allowed to interact during 10 min at 4 °C. Hereafter, the surfactant coat was formed by high-energy sonication as described above.

2.4. Fluorescence single particle tracking

Fluorescence single particle tracking (fSPT) is a technique that monitors the diffusional movement of individual fluorescently labeled particles using a highly sensitive fluorescence microscope setup [33]. This technique allows to accurately measure size distributions of nanoparticles dispersed in complex biological fluids. In our experiments, a swept-field confocal microscope (LiveScan Swept Field Confocal Microscope System; Nikon, Brussels, Belgium) was used. Briefly, a solid-state 125 mW 640 nm (Agilent Technologies, CA, USA) laser was used to excite the fluorophore in samples mounted on the microscope equipped with a Plan Apo VC 100x 1.4 NA oil immersion objective lens (Nikon). A fast and sensitive EMCCD camera (Ixon Ultra 897; Andor Technology, CT, USA) enables recording high-speed confocal movies of individual diffusing particles. Single particle trajectories, and corresponding diffusion coefficients, were subsequently calculated using in-house developed software, which is explained in detail elsewhere [34].

In this work, fSPT was used to compare the size distributions of siNGs and surfactant-coated siNGs prepared *via* the protocols described above. Hereto, the NGs were first loaded with Cy5-labeled siRNA (10 pmol siRNA per µg NGs), allowing to specifically monitor the movements of the fluorescent NGs without interference of the non-labeled surplus Curosurf® vesicles present in the dispersion. The nanoparticles were diluted in HEPES buffer (pH 7.4, 20 mM) or in Opti-MEM® (Gibco®- Life Technologies) to give a concentration suitable for fSPT (typical concentrations of 10^8–10^{10} particles per mL). A total of 5 µL of these samples was then applied between a microscope slide and a cover glass with a double-sided adhesive sticker of 120 µm thickness in between (Secure-Seal Spacer, Molecular Probes, Leiden, The Netherlands). The microscope was always focused 20 µm above the cover glass. For each sample, 20 movies of approximately 200 frames each were recorded at different random locations within the sample, mounting to 1600-2400 individual particle trajectories per sample.

2.5. Fluorescence fluctuation spectroscopy

Fluorescence fluctuation spectroscopy (FFS) monitors fluorescence intensity fluctuations in the excitation volume of a confocal microscope. The fluorescence fluctuations originate from the movement of fluorescent molecules in and out a fixed excitation volume. FFS measurements were performed with a laser scanning confocal microscope (C1si, Nikon) equipped with a water immersion objective lens (Plan Apo 60X, NA 1.2, collar rim correction, Nikon), using a 637 nm laser line for the excitation of fluorescent siRNA (siCy5). The latter setup was combined with the detection channels of the fluorescence correlation spectrometer MicroTime 200 (Picoquant GmbH, Berlin, Germany), equipped with SymPhoTime software.

In previous work by our group, FFS was used to quantify the complexation of fluorescently labeled siRNA to e.g. cationic liposomes or polymers [13, 35-37]. In this study, FFS experiments were carried out on dextran nanogels loaded with Cy5-labeled siRNA. First, the maximal loading capacity of the pre-formed NGs for siRNA was assessed by mixing increasing NG concentrations with a fixed amount of fluorescent siRNA. Next, the release of siRNA from the siNGs was evaluated before and after coating with Curosurf® in the presence of competing polyanions, i.e. dextran sulfate sodium salt (DEXS, 10 kDa, Sigma-Aldrich) or mucin (from porcine stomach-type II, Sigma-Aldrich). Equal volumes of these strongly negatively charged polymers (in HEPES buffer or PBS) were mixed with the nanoparticles, resulting in a final siRNA concentration of 25 nM. After 10 min incubation at room temperature the samples were transferred to a glass-bottomed 96-well plate (Greiner Bio-one GmbH, Frickenhausen, Germany). Subsequently, the focal volume of the microscope was positioned in the sample and the fluorescence fluctuations were recorded during a 60 s time interval. All samples were prepared in triplicate. The average fluorescence intensity of freely

diffusing and complexed siRNA in the fluorescence fluctuation profile was determined as described previously [37].

2.6. Cryogenic transmission electron microscopy

Cryogenic transmission electron microscopy (cryo-TEM) is a valuable tool for the structural investigation of nanosized particles [38]. Both NGs and Curosurf® vesicles were diluted in HEPES buffer (final concentration of respectively 5 and 10 mg mL^{-1}). The Curosurf® vesicles were formed by sonication of the crude surfactant dispersion using a probe sonicator (amplitude 10 %; Branson). Coated nanogels were formed according to the method described above. The ratio of surfactant to NGs equaled 7.5 mg Curosurf® / mg NGs. 2.5 µL of the different samples was placed on a glow discharged holey carbon coated grid (Quantifoil® R 3.5/1, Quantifoil Micro Tools GmbH, Grosslöbichau, Germany). The excess of liquid was blotted with a filter paper, reducing the droplet to a thin film. The samples were vitrified in liquid ethane, using a vitrobot (FEI, Eindhoven, The Netherlands) and stored in liquid nitrogen until observation. The grids were transferred to a cryo specimen holder type 626 (Gatan GmbH, München, Germany) and observed in a CM 120 cryo-electron microscope (Philips, Eindhoven, The Netherlands) operating at 120 keV. Images were recorded on a slow-scan CCD camera (Gatan GmbH) under low-dose conditions.

2.7. Preparation of folate-targeted surfactant-coated nanogels

1,2-distearoyl-sn-glycero-3-phosphoethanolamine-N-[folate(polyethylene glycol)-2000] (ammonium salt) (DSPE-PEG_{2000}-folate) was purchased from Avanti Polar Lipids, Inc. (AL, USA). To incorporate folate as a targeting ligand in the pulmonary surfactant layer, Curosurf® and DSPE-PEG_{2000}-folate were mixed in chloroform:methanol (2:1) at different weight ratios. A lipid film was formed by rotary evaporation of the organic solvents under vacuum at 37 °C. The dried lipid film was rehydrated in HEPES buffer under mechanical agitation, resulting in a final lipid concentration of 4.5 mg mL^{-1}. This hydrated lipid film was used in the coating procedure, as described above. To assess the influence of DSPE-PEG_{2000}-folate on the particle size, size distribution of the hybrid nanoparticle upon inclusion of the folate ligands was determined in HEPES buffer using fSPT. Additionally, siRNA release profiles in HEPES or mucin were quantified by FFS.

2.8. Cell lines and culture conditions

Cell culture experiments were performed using human alveolar epithelial cells (H1299), H1299 cells that stably express the EGFP (H1299_EGFP), and human lung adenocarcinoma cells (A549). H1299 and A549 cells were cultured in RPMI 1640 and DMEM, respectively, supplemented with 2 mM glutamine, 10 % fetal bovine serum and 100 U mL^{-1} penicillin/streptomycin at 37°C in a humidified atmosphere containing 5 % CO_2. Cells were passed every 3 days using 0.25 % trypsin- ethylenediaminetetraacetic acid solution in order to maintain sub-confluency. H1299_EGFP cells were treated with medium containing 1 mg mL^{-1} Geneticin® once per month for selection. All materials were purchased from Gibco®-Life Technologies, except for the serum, which was delivered by Hyclone™ (Thermo Fisher Scientific).

2.9. Quantification of siRNA cellular internalization by flow cytometry

To quantify the cellular uptake of siRNA by flow cytometry in the lung epithelial cells, H1299_EGFP and A549 cells were seeded in 24-well plates (Greiner Bio-One GmbH) at a density of 1.85 x 10^4 cells cm^{-2} and 2.10 x 10^4 cells cm^{-2} respectively. After 24 h, the cells were incubated for 4 h (37 °C, 5 % CO_2) with the different formulations described below.

NGs were loaded with different amounts of siRNA, labeled with 0.75 mol% Cy5 and coated with Curosurf® using the coating procedure described above. According to the experimental needs, different weight ratios of DSPE-PEG_{2000}-folate were incorporated in the pulmonary surfactant, before initiating the coating procedure. After five-fold dilution in Opti-MEM®, resulting in a final NG concentration of 30 μg mL^{-1}, the samples were incubated with the cells. Following incubation, the cells were washed with PBS supplemented with DEXS (0.1 mg mL^{-1} in PBS) to remove surface-bound fluorescence. Next, the cells were harvested in 250 μL flow buffer (PBS supplemented with 1 % bovine serum albumin and 0.1 % sodium azide) and placed on ice until flow cytometric analysis. Transfections were performed in triplicate and a minimum of 10^4 cells was analyzed in each measurement, using a FACSCalibur™ flow cytometer (BD Biosciences, Erembodegem, Belgium). The fluorescence detector for Cy5-labeled siRNA detects wavelengths of 661 nm (±16 nm). Data analysis was performed using the CellQuest Pro™ analysis software (BD Biosciences).

2.10. Quantification of EGFP silencing by flow cytometry

H1299_EGFP cells were plated in 24-well plates (1.85 x 10^4 cells cm^{-2}). NGs were loaded with variable amounts of siCTRL or siEGFP. Next, the siNGs were coated with Curosurf®. Depending on the experimental needs, different weight ratios of DSPE-PEG_{2000}-folate were incorporated in the pulmonary surfactant layer. After five-fold dilution in Opti-MEM®, the samples were brought onto the cells. Following 4 h of incubation at 37 °C and 5 % CO_2, non-internalized nanoparticles were removed and the cells were incubated with 1 mL fresh cell culture medium for 48 h. Cells were prepared for analysis by flow cytometry as described above. Transfections were performed in triplicate and a minimum of 10^4 cells was analyzed in each measurement.

2.11. Visualization of lysosomal colocalization by confocal microscopy

H1299 cells were seeded in a 35 mm culture dish (Greiner Bio-One GmbH) at a density of 2.0 x 10^4 cells cm^{-2} and allowed to attach overnight. The cells were incubated with NGs, coated NGs-2, or coated NGs-2 folate (incorporating 7.5 wt% folate in the outer surfactant shell) complexed with fluorescent siRNA (siCy5; 10 pmol siCy5 per μg NG) during 2 h. Subsequently, the cells were washed with PBS and incubated in preheated culture medium during 1 h. Prior to lysosomal staining, the cells were fixed (4 % paraformaldehyde in PBS) and permeabilized (0.5 % Tween 20 in PBS) at room temperature. After three washing steps with blocking buffer (5 % goat serum in PBS), the cells were incubated with a primary antibody against lysosomal-associated membrane protein-1 (LAMP-1; Sigma-Aldrich). After incubation with the secondary antibody (Alexa Fluor® 488 labeled goat anti-rabbit IgG; Life Technologies), cell nuclei were stained with Hoechst (Life Technologies) and the cells were mounted with Vectashield® Mounting Medium (Vector Labs, Peterborough, United Kingdom). The intracellular fluorescence distribution was visualized with a laser scanning confocal microscope (C1si, Nikon). The confocal images were captured with a Nikon Plan Apo 60x oil immersion objective using a 488 nm and 637 nm laser line for the excitation of Alexa Fluor® 488-labeled lysosomes and the Cy5-labeled siRNA respectively.

An object-based colocalization algorithm was used to quantify the number of siRNA-loaded particles that are located inside lysosomes. First, the siCy5 loaded particles were identified in the red image by intensity thresholding. Only “objects” consisting of at least 8 pixels were retained. The thresholded image was then binarized in order to generate a mask for superposition on the corresponding green image (containing the Alexa Fluor®488 stained lysosomes). This allows to calculate the green (lysosomal) intensity *G* for each object. Next, the background intensity (mean value *BG* and standard deviation *S*) of the cell in the image

was determined within a rectangular area not containing any lysosomes. Finally, a siCy5-loaded particle is decided to be colocalized with a lysosome if its green intensity $G > BG+S$.

2.12. Statistical analysis

All data are presented as mean ± standard deviation (n=3). Statistical analyses were performed by one-way ANOVA with Bonferroni correction or by an unpaired t-test, using GraphPad Prism software version 6.

3. Results

3.1. Optimizing the protocols for the development of pulmonary surfactant-coated nanogels

The key objective of this study was to design bio-inspired hybrid nanoparticles for pulmonary siRNA delivery, capable of overcoming lung-specific barriers. We envisioned core-shell nanocomposites, consisting of a cationic biodegradable dextran nanogel (NG) core that is loaded with siRNA (siRNA-loaded NG; siNG) and layered with a pulmonary surfactant shell. The cationic NG core was produced *via* an inverse mini-emulsion photopolymerization of methacrylated dextran and a methacrylated monomer containing a quaternary amine moiety [13]. A commercially available pulmonary surfactant, derived from minced porcine lungs (i.e. Curosurf®), was used to construct the surfactant shell. The pulmonary surfactant-coated siNGs (coated siNGs) were fabricated *via* two distinct protocols, which are depicted in **Figure 1**. Both protocols encompass a two-step synthesis, wherein the first step involves the encapsulation of siRNA into the NGs based on electrostatic interaction, as described earlier by Raemdonck et al. [13]. **Figure S1** shows that the NGs used in this study exhibit a high loading capacity for siRNA exceeding 30 pmol siRNA per µg NGs. This corresponds to ≥ 50 wt% loading and corroborates earlier findings [13]. In order to ensure complete complexation of siRNA, a siRNA loading of < 20 pmol μg^{-1} was employed. The second step, in which the pulmonary surfactant is layered around the siNG core, can be achieved using two different mixing methods. One approach is to initially homogenize the original pulmonary surfactant dispersion, comprising micron-sized lipid aggregates, by probe sonication to form unilamellar anionic surfactant vesicles with a hydrodynamic diameter and zeta-potential of ~ 80 nm and ~ -35 mV, respectively (data not shown). Next, the cationic siNGs and the anionic surfactant vesicles are combined, resulting in the electrostatic adsorption of the surfactant vesicles on the NG surface. The obtained dispersion of hybrid nanoparticles *via* this approach is hereafter abbreviated as *coated siNGs-1* (**Figure 1a**). In the alternate approach, the pre-formed siNGs are directly mixed with the crude pulmonary surfactant dispersion, after which probe sonication is applied. The high-energy input in this step may facilitate lipid reorganization around the NG surface, resulting in a composite nanoparticle further denoted as *coated siNGs-2* (**Figure 1b**).

3.2. The pulmonary surfactant shell enhances the colloidal stability of the siRNA-loaded nanogels

The influence of both coating procedures on the size of the resultant composite formulations was determined. It is important to note that the preparation protocol of the surfactant-coated siNGs requires an excess of pulmonary surfactant to avoid aggregation. However, the latter implies that two distinct nanoparticle populations are likely present in the pulmonary surfactant-coated siNG dispersion: (i) the coated siNGs, and (ii) an excess of empty surfactant vesicles. The surplus of surfactant vesicles will interfere with the size determination of the coated siNGs when using conventional techniques based on light scattering. Unlike these methods, fluorescence single particle tracking (fSPT) allows to measure an accurate size distribution of fluorescently labeled nanoparticles in complex heterogeneous mixtures [33].

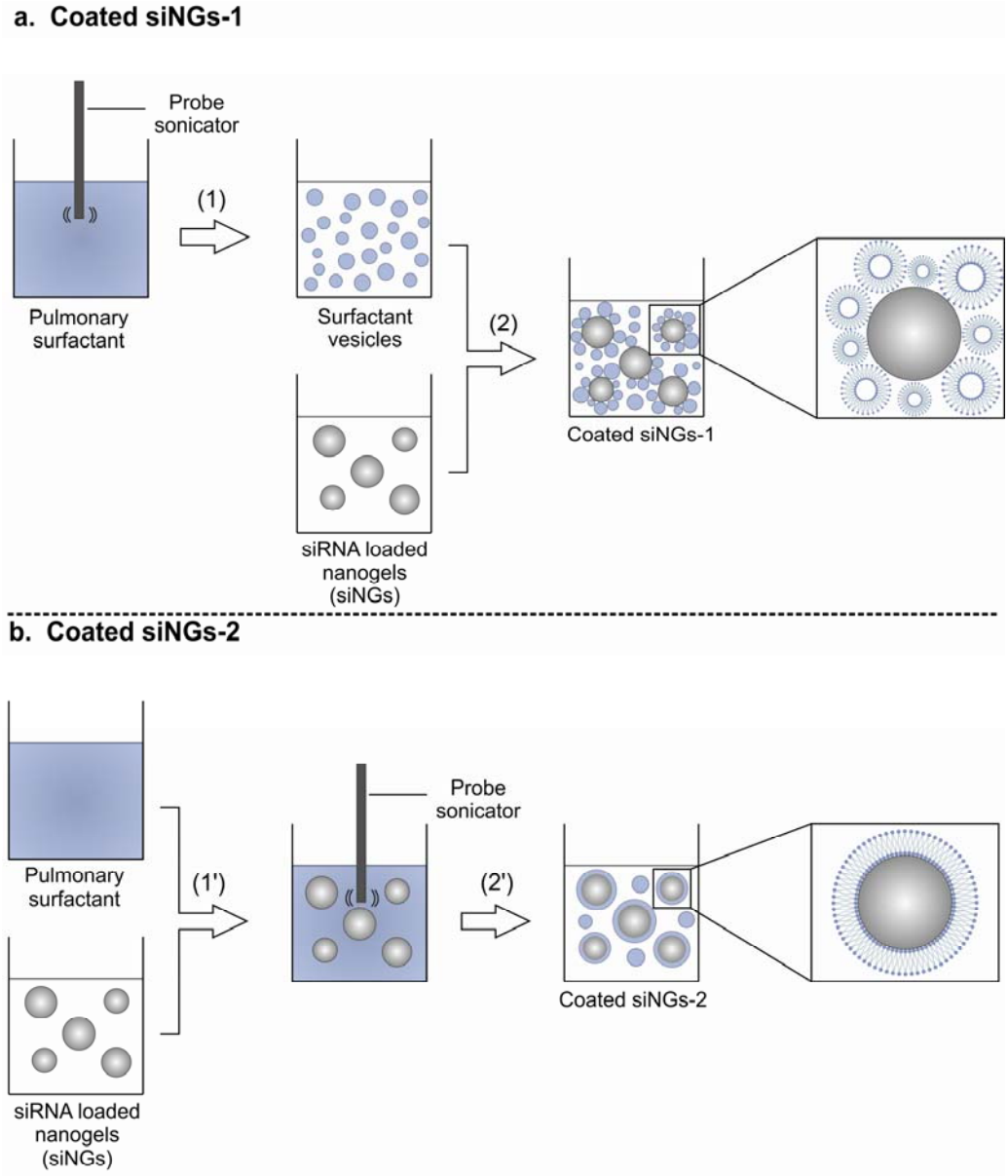

Figure 1. Scheme illustrating the synthesis of pulmonary surfactant-coated siRNA-loaded nanogels (coated siNGs). Two distinct protocols were evaluated of which the different steps are shown. **(a)** First approach showing (1) the formation of unilamellar surfactant vesicles by probe sonication and (2) the electrostatic interaction between the pre-formed siNGs and the surfactant vesicles. **(b)** Second approach showing (1') the interaction between the pre-formed siNGs and the unprocessed surfactant dispersion and (2') the induction of phospholipid fusion onto the nanogel surface *via* probe sonication.

This technique, developed by our group, was used to determine the size of the coated siNGs. The NG core was loaded with fluorescently labeled siRNA (siCy5), allowing to specifically determine the size distribution of the coated siNGs without interference of the excess non-labeled surfactant vesicles present in the dispersion (**Figure 2**).

The uncoated siNGs have an average hydrodynamic diameter around 200 nm as measured in HEPES buffer (**Figure 2a**). The interaction of the siNGs with Curosurf® vesicles (coated siNGs-1), resulted in a two-fold increase in size. In contrast, the hybrid nanoparticles that were fabricated *via* the alternate protocol (coated siNGs-2) have an average size of 230 nm. The size distributions shown in **Figure 2a** were measured in a low salt buffer. As the presence of salt can have an important impact on the physicochemical characteristics of charged

nanoparticles, it is crucial to also evaluate their size in isotonic media. **Figure 2b** shows the size distribution of the different formulations in Opti-MEM®. The hydrodynamic size of the uncoated siNGs was markedly shifted to larger values, which is indicative of aggregation. This observation is in stark contrast to both surfactant-coated formulations, of which the average size remains largely unaffected.

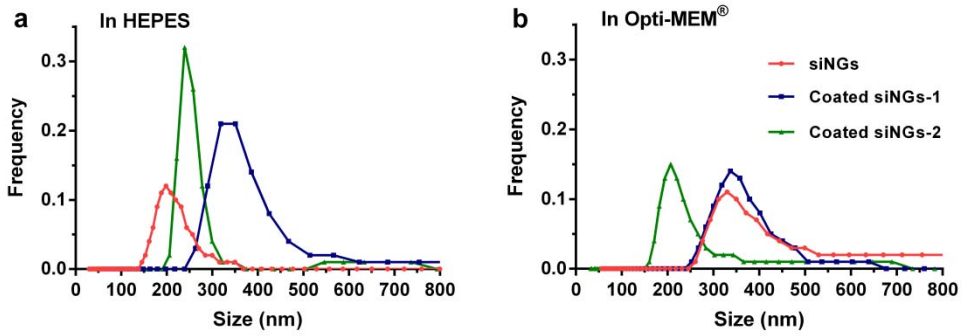

Figure 2. Size distributions of the uncoated siRNA-loaded nanogels (siNGs) and the surfactant-coated siNGs, as determined by fluorescence single particle tracking. The nanogels (NGs) were loaded with 10 pmol of fluorescently labeled siRNA (siCy5) per µg NGs. The experiments were performed at room temperature in HEPES buffer (pH 7.4, 20mM) **(a)** or Opti-MEM® **(b)**.

3.3. The pulmonary surfactant shell prevents premature release of siRNA from the nanogel core

Nanocarriers relying on electrostatic complexation for siRNA loading are particularly prone to dissociation of siRNA from the carrier following interaction with other polyanionic molecules, resulting in premature siRNA release in the extracellular matrix prior to reaching the intracellular site-of-action [35, 39]. The siRNA release profiles in the presence of competing polyanions should therefore be investigated. Here, the strongly negatively charged polymers dextran sulfate (DEXS) and mucin were used. The influence of the pulmonary surfactant shell on the release of siRNA from the NG core was assessed upon 10 min of incubation with these polyanions, using fluorescence fluctuation spectroscopy (FFS). The feasibility of FFS to quantify siRNA complexation and release has already been demonstrated by our group for various types of nanocarriers [35-37].

Figure 3a indicates that mucin, starting from 0.5 mg mL^{-1}, caused an almost complete release of the siRNA from the uncoated siNGs. Likewise, complexed siRNA was also fully released from the coated siNGs-1 formulation. In contrast, coated siNGs-2 could partially prevent the siRNA release, reaching a maximal release of 55 ± 2% in the presence of 1 mg mL^{-1} mucin. Increasing the sonication time in the synthesis protocol did not confer additional protection against siRNA release (**Figure S2**). On the other hand, increasing the siRNA loading of the NGs up to 20 pmol siRNA per µg NG resulted in an added release of siRNA from the coated siNGs-2 (**Figure S2**). Based on these results, further experiments were performed with the coated siNGs-2 formulation with ≤ 10 pmol siRNA loading per µg NG.

Next, the impact of the surfactant-to-NG ratio on the siRNA release from the coated siNGs-2 was determined. As can be seen in **Figure 3b**, no significant siRNA release could be detected prior to the addition of the competing polyanions. This implies that the decoration of the siNGs with the negatively charged pulmonary surfactant shell did not significantly induce a siRNA release, even at high weight excess of the surfactant. As expected, the siRNA was almost completely released from the uncoated siNGs in the presence of two destabilizing polyanions, i.e. mucin or DEXS (**Figure 3b**). Strikingly, applying a 5-fold weight excess of surfactant during the coating procedure could already reduce the siRNA release to maximally 58 ± 4% or 48 ±7% in the presence of DEXS or mucin, respectively. When further increasing

the surfactant-to-NG ratio up to a 15-fold weight excess of surfactant, the protection against siRNA release was significantly improved. Here, siRNA release was limited to 52 ± 4% or 33 ± 4% in the presence of DEXS or mucin, respectively. A ratio of 15 mg surfactant per mg NG was therefore selected for subsequent experiments.

Likely, the presence of salt during the coating procedure could also have a significant impact on the structure of the surfactant shell. In **Figure 3c** it was confirmed that mixing pulmonary surfactant and siNGs in medium with low ionic strength (HEPES buffer) confers improved resistance against siRNA displacement by a destabilizing agent (i.e. mucin). However, preparing the coated siNGs in media with higher ionic strength (PBS) resulted in a complete release of siRNA following the addition of 2.5 mg mL^{-1} mucin. This can most likely be attributed to a charge screening effect in media with higher ionic strength, reducing the electrostatic interaction between the cationic siNGs and the anionic surfactants, which is clearly the driving force behind the lipid coating process.

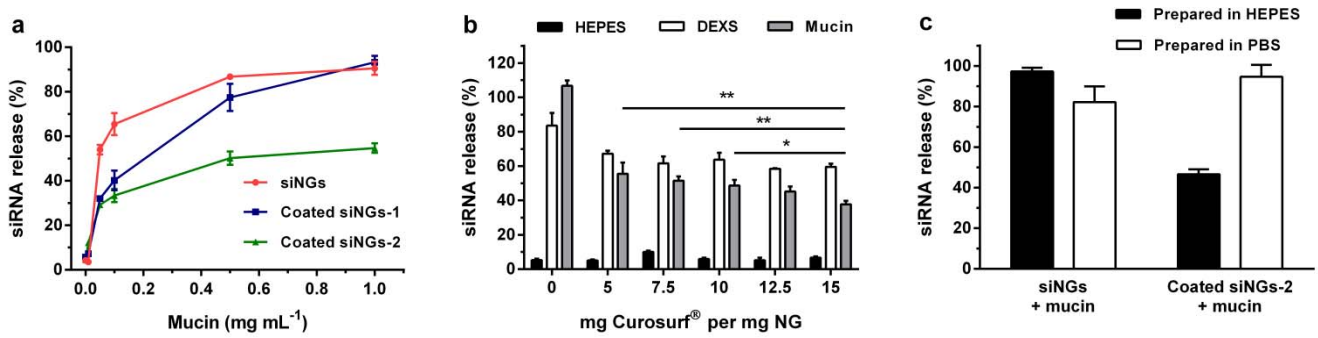

Figure 3. Influence of the pulmonary surfactant shell on the siRNA release in the presence of competing polyanions, as measured by fluorescence fluctuation spectroscopy. (a) Comparison of the siRNA release from the uncoated siRNA-loaded NGs (siNGs) or surfactant-coated siNGs (15 mg surfactant per mg NG) at varying concentrations of mucin in HEPES buffer (pH 7.4, 20mM). **(b)** siRNA release from coated siNGs-2 in HEPES buffer (black bars), and in the presence of dextran sulfate (2.5 mg mL^{-1}; white bars), or mucin (2.5 mg mL^{-1}; gray bars). **(c)** Release of siRNA from the uncoated siNGs and coated siNGs-2 (15 mg surfactant per mg NG) *prepared* in HEPES buffer (black bars) or *prepared* in PBS (white bars). The percentage released siRNA was determined in the presence of mucin (2.5 mg mL^{-1} in HEPES buffer or PBS, respectively). The concentration of fluorescent siRNA equaled 25 nM in all samples. Nanogels (NGs) were loaded with 10 pmol siRNA per µg NGs. Data points represent mean ± standard deviation (n=3, * $p \leq 0.05$, ** $p \leq 0.01$)

3.4. Investigating the morphology of the pulmonary surfactant-coated nanogels

Cryogenic transmission electron microscopy (cryo-TEM) was used to visualize the morphology of the composite nanoparticles. The cryo-TEM images of the uncoated siNGs display spherical particles with a clear porous structure and a diameter between 100 and 200 nm (**Figure 4a**), which is in line with the hydrodynamic diameter measured by fSPT. Curosurf® vesicles appear as unilamellar and spherical liposomes with a faceted surface, which is attributed to the high content of dipalmitoylphosphatidylcholine (DPPC) in the Curosurf® formulation (**Figure 4b**) [40].

As expected based on the excess of pulmonary surfactant used in the synthesis protocol, cryo-TEM imaging of the coated siNGs-2 dispersion revealed two co-existing nanostructures. In addition to the coated siNGs-2, which show a core-shell nanoarchitecture comprising the NG core enveloped by a unilamellar surfactant shell (**Figure 4c**, marked by the white arrows), also an excess of empty Curosurf® vesicles can be observed. It is important to note that in the dispersion of coated siNGs-2, every detected siNG particle appeared to be decorated with a surfactant outer shell. However, some nanoparticles clearly showed defects in the surrounding

lipid bilayer (**Figure S3**; white arrow), indicating that the surfactant coating procedure does not guarantee the formation of a perfectly uniform lipid shell for every core nanoparticle.

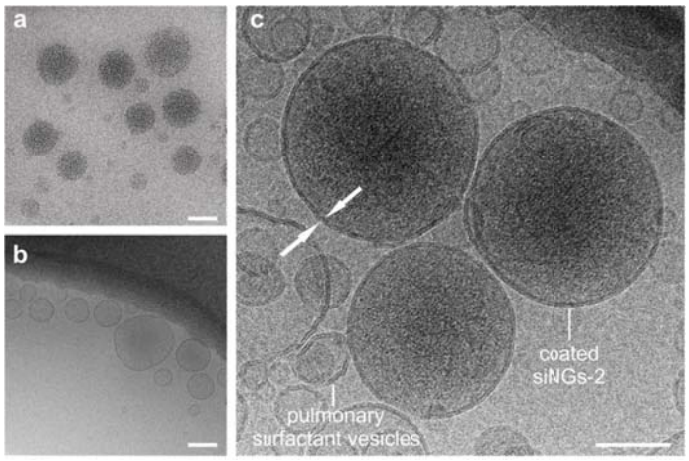

Figure 4. Morphological characterization by cryogenic transmission electron microscopy (cryo-TEM). Cryo-TEM images of the uncoated siRNA-loaded nanogels (siNGs) **(a)**, Curosurf® vesicles **(b)**, and the coated siNGs-2 **(c)**. The white arrows mark the surfactant coat. Scale bars correspond with 100 nm.

3.5. The pulmonary surfactant shell potentiates the intracellular siRNA delivery in lung cancer cells

Prior to testing the biological efficacy, we assessed the acute cytotoxicity of the different formulations on a lung epithelial carcinoma cell line (H1299_EGFP). Exposing these cells to siNGs, Curosurf® vesicles, pulmonary surfactant-coated siNGs (coated siNGs-2) did not cause a significant reduction in cell viability (**Figure S4**).

Next, the cellular uptake and gene silencing potential of the optimized hybrid formulation was quantified by flow cytometry in H1299_EGFP cells that stably express the EGFP gene. The presence of a pulmonary surfactant outer shell significantly lowered cellular internalization of the siNGs, reducing the intracellular dose of fluorescently labeled siRNA with ~80 % (**Figure 5a**). Remarkably, the EGFP silencing obtained with the hybrid formulation remained unaffected when compared to the uncoated siNGs. At the highest siRNA dose (100 nM), coated siNGs-2 even outperformed the uncoated siNGs (**Figure 5b**; $p < 0.05$, unpaired t-test).

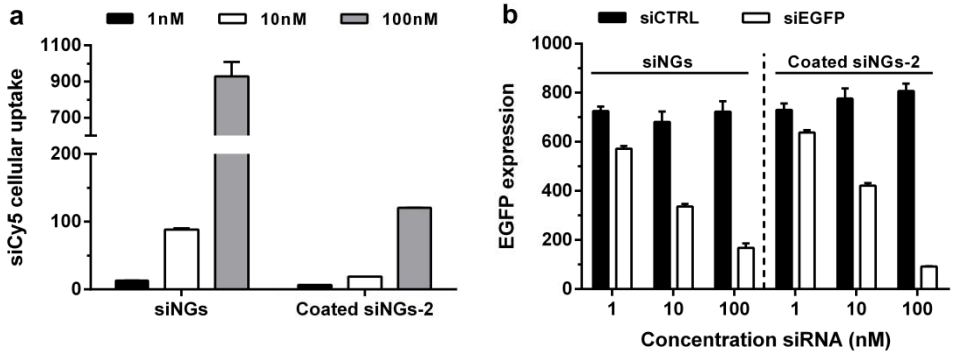

Figure 5. Influence of the pulmonary surfactant shell on the cellular uptake and gene silencing potential of siRNA-loaded nanogels (siNGs) in H1299_EGFP cells, determined by flow cytometry. The experiments were performed with a fixed nanogel concentration per well (30 µg mL^{-1}), while the siRNA concentrations varied from 1 nM to 10 nM and 100 nM per well. **(a)** Cellular uptake of NGs loaded with fluorescent siRNA (0.75 mol% Cy5-labeled). **(b)** Evaluation of EGFP silencing by uncoated siNGs and coated siNGs-2. The NGs were loaded with control siRNA (siCTRL) or active siRNA (siEGFP). Data points represent the mean fluorescence intensities ± standard deviation (n=3).

3.6. Incorporation of a targeting ligand enhances the efficacy of the pulmonary surfactant-coated nanogels

Besides stabilizing the nanocarrier in the extracellular compartment and guiding intracellular siRNA delivery, the surfactant shell may impart other valuable traits, such as the straightforward inclusion of targeting ligands. One of the most extensively studied targeting moieties for drug delivery is folate. The folate receptor α (FR) is frequently overexpressed in a range of tumor cells [41]. Folate specifically binds to FR with a high affinity, making it a prime candidate for active targeting of nanoparticles. In our work, DSPE-PEG_{2000}-folate, a PEGylated lipid carrying a folate group at its distal end, was incorporated in the pulmonary surfactant layer at different weight ratios (**Figure 6a**). First, we evaluated whether the incorporation of DSPE-PEG_{2000}-folate influences the size of the hybrid nanoparticles. Incorporation of 10 wt% DSPE-PEG_{2000}-folate only caused a minor shift in size distribution (**Figure S5_a**), most likely attributed to the presence of PEG chains on the particle surface. Likewise, the extent of siRNA release in the presence of mucin was largely independent of the inclusion of the folate-modified lipids (**Figure S5_b**). From these data we can conclude that the addition of up to 10 wt% of PEGylated and folate-modified lipids in the surfactant shell does not alter the physicochemical characteristics of the hybrid formulation.

Before the impact of the folate targeting ligand on the cellular uptake of the coated nanoparticles was assessed, it was confirmed that the incorporation of folate in the outer surfactant shell did not induce acute cytotoxicity (**Figure S4**). **Figure 6b** shows a gradual increase of internalized siRNA in H1299_EGFP cells, which overexpress the FR, as a function of the surface density of folate groups. Remarkably, a sudden rise in cellular siRNA dose was observed from 5 to 7.5 wt% DSPE-PEG_{2000}-folate with no further improvement in cellular uptake at 10 wt% of folate modified lipids.

To demonstrate the specificity of the folate targeting, the cellular uptake of the different formulations was quantified in A549 cells, which do not overexpress the folate receptor (**Figure 6c**) [41]. The uncoated siNGs were equally well internalized by A549 cells as compared to H1299_EGFP cells. In addition, coating the siNGs with pulmonary surfactant also substantially impaired cellular uptake in A549 cells, reducing the intracellular siRNA dose with > 85%. Importantly, only a negligible increase in siRNA fluorescence could be detected in A549 cells with the optimized folate-targeted core-shell formulation. This is in stark contrast to the four-fold induction in intracellular siRNA fluorescence obtained in H1299_EGFP cells with the same formulation, confirming the involvement of a specific receptor-mediated uptake mechanism. To evaluate if the enhanced cellular internalization also results in an improved RNAi effect, we quantified the EGFP gene silencing in H1299_EGFP cells obtained with coated siNGs-2 as a function of wt% DSPE-PEG_{2000}-folate inclusion (**Figure 6d**). The magnitude of EGFP silencing is markedly enhanced for the targeted formulations and clearly correlates with the observed improvement in cellular uptake (**Figure 6b**). Incorporating 7.5 wt% DSPE-PEG_{2000}-folate in the surfactant shell reduced EGFP expression with 80 % at a low siRNA concentration of 5 nM, compared to only ~20% silencing obtained without the folate targeting ligand. Increasing the fraction of folate-modified lipids to 10 wt% did not further enhance the gene knockdown, which is also in line with the cellular uptake data.

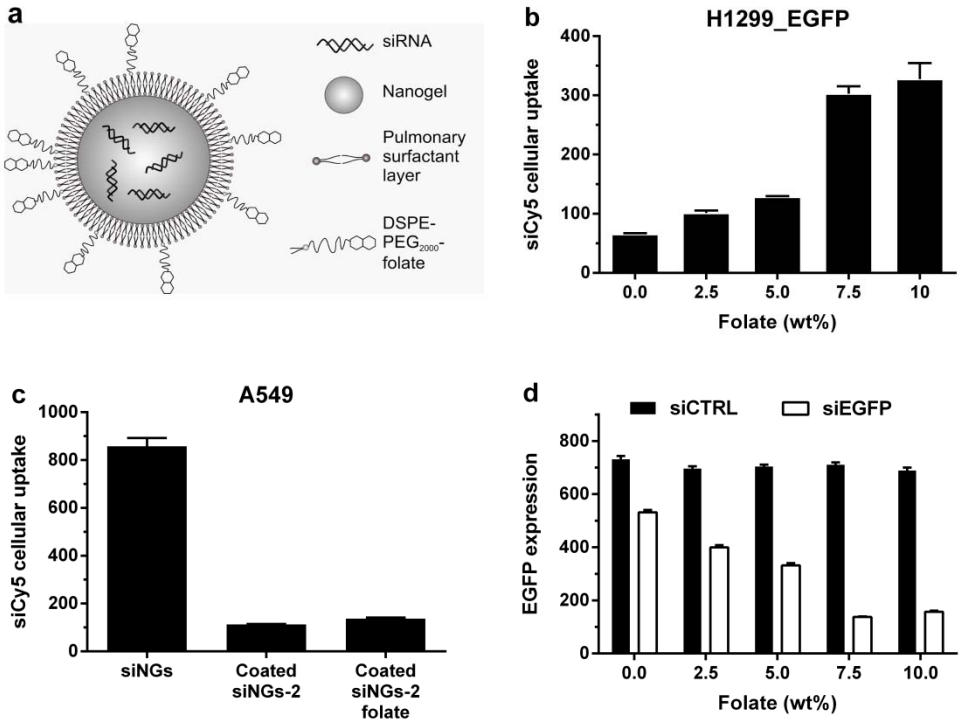

Figure 6. Influence of the folate targeting ligand on the cellular uptake and gene silencing potential of the hybrid nanoparticles. (a) Schematic representation of the surfactant-coated siRNA-loaded nanogels (coated siNGs-2) incorporating folate-modified phospholipids in the pulmonary surfactant outer shell. **(b)** Cellular uptake in H1299_EGFP cells, which overexpress the folate receptor α (FR), of coated siRNA-loaded nanogels (coated siNGs-2) as a function of the weight ratio of DSPE-PEG_{2000}-folate. **(c)** Cellular uptake of uncoated siNGs, coated siNGs-2 and coated siNGs-2 incorporating 7.5 wt% folate in A549 cells, which do not overexpress FR. **(d)** Evaluation of EGFP silencing by coated siNGs-2 incorporating different folate weight ratios in H1299_EGFP cells. The NGs were loaded with control siRNA (siCTRL) or active siRNA (siEGFP). The experiments were performed with a fixed NG concentration (30 µg mL^{-1}). Every well contained 5 nM siRNA. For the uptake experiments fluorescent siRNA was used (0.75 mol% Cy5-labeled). Data points represent mean fluorescence intensities ± standard deviation (*n*=3).

3.7. Elucidating the intracellular fate of the pulmonary surfactant-coated nanogels

In order to assess the impact of the pulmonary surfactant outer shell on the intracellular fate of the nanoparticles, we performed a colocalization experiment via confocal fluorescence microscopy. Here, a specific labeling of the lysosomes was obtained by immunofluorescence staining of the lysosomal-associated membrane protein-1 (LAMP-1). H1299 cells were incubated with fluorescently labeled siRNA (siCy5) complexed with uncoated nanogels (siNGs), coated NGs (coated siNGs-2), or coated NGs-2 incorporating 7.5 wt% DSPE-PEG_{2000}-folate (coated siNGs-2 folate). The confocal images clearly show a punctuated siCy5 fluorescence which is indicative of endocytic uptake (Figure 7). The observed differences in intracellular siCy5 fluorescence between the formulations confirm our data obtained with flow cytometry. Moreover, the images clearly illustrate colocalization of the red-labeled nanoparticles and the green-labeled lysosomes. In addition, we performed a detailed colocalization analysis using appropriate image processing software. This analysis revealed that ~80 % of the siNGs were colocalized with the lysosomes. Importantly, the presence of a pulmonary surfactant outer shell, with or without incorporated folate-modified lipids, did not significantly alter the extent of lysosomal sequestration.

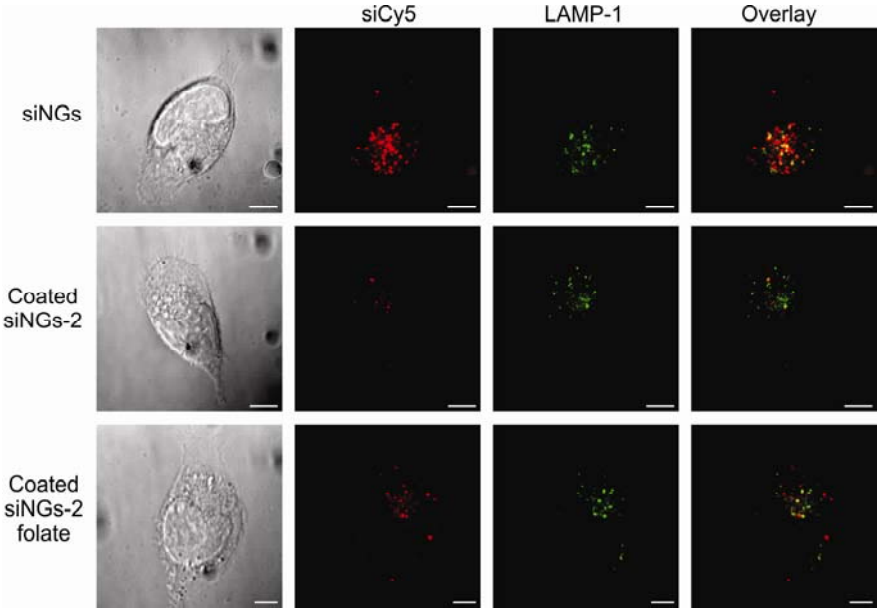

Figure 7. Confocal images of fluorescent siRNA (siCy5) complexed with nanogels (siNGs), pulmonary surfactant-coated NGs (coated siNGs-2) or coated NGs incorporating 7.5 wt% folate (coated siNGs-2 folate) in H1299 cells. A specific labeling of lysosomes was obtained by immunofluorescence staining against lysosomal-associated membrane protein-1 (LAMP-1). The experiments were performed with a fixed nanogel (NG) concentration (30 µg mL^{-1}) complexed with 10 pmol siCy5 per µg NG. Scale bars correspond with 10 µm.

4. Discussion

In this study, we have successfully designed a targeted composite nanocarrier composed of a siRNA-loaded dextran nanogel (siNG) core and a pulmonary surfactant shell. Hybrid nanoparticles, combining the benefits of both polymer- and lipid-based nanoparticles within a single delivery vehicle, have emerged as a promising drug delivery platform [14-16]. A number of examples have been described in the literature that highlight the potential of such hybrid nanoparticles for siRNA delivery upon systemic application [17, 18]. However, their value for pulmonary siRNA delivery was not yet evaluated. In addition, although synthetic drug carriers are being actively developed for many applications, a growing interest exists in the implementation of bio-inspired materials in drug delivery [22, 23].

We evaluated two distinct protocols to synthesize surfactant-coated siNGs. Hybrid nanoparticles prepared *via* the coated siNGs-2 protocol (**Figure 1b**) clearly outperformed the nanoparticles prepared *via* the coated siNGs-1 protocol (**Figure 1a**) in terms of safeguarding the siRNA payload in the presence of a destabilizing agent (i.e. mucin). Likely, the electrostatic interaction between the siNGs and preformed Curosurf® vesicles (coated siNGs-1) does not allow optimal fusion of surfactant lipids on the NG surface, as also evidenced by the large shift in hydrodynamic diameter (**Figure 2**). The observed shift in size will likely correspond with the mere electrostatic attachment of surfactant vesicles to the NG surface, given the average diameter of ± 80 nm, as measured for the Curosurf® vesicles. The absence of an effective fusion of the surfactant vesicles on the NG surface is in contrast with earlier reports on mesoporous silica nanoparticles for which incubation with anionic liposomes led to spontaneous fusion of the liposomes on the nanoparticle surface [42]. On the other hand, coated siNGs-2 nanoparticles, have a hydrodynamic size that more closely resembles the size of the original siNG core (**Figure 2**) and cryo-TEM analysis confirmed the presence of a single surfactant bilayer on the NG surface for the majority of nanoparticles (**Figure 4**). We hypothesize that the high-energy sonication provides enough shear force to facilitate lipid reorganization around the nanoparticle surface. Nevertheless, the pulmonary surfactant shell

did not completely block siRNA release from the NG core in the presence of strongly negatively charged polymers, such as mucin and dextran sulfate (**Figure 3a**). This can possibly be attributed to defects in the pulmonary surfactant shell, as observed for some particles in the cryo-TEM images (**Figure S3**), allowing the diffusion of the polyanions into the NG core and subsequent siRNA displacement.
The electrostatic interaction between the siNG core and the pulmonary surfactant shell appeared to be the predominant factor driving the coating process. This was clearly reflected by the inability to prepare stable core-shell nanoparticles in the presence of isotonic salt concentrations (**Figure 3c**). The higher ionic strength, compared to HEPES buffer, enhanced the shielding of the surface charges, thereby significantly decreasing the electrostatic interaction between the siNGs and pulmonary surfactant.
In previous work by our group, it was already illustrated that pulmonary surfactant could potentiate intracellular siRNA delivery [29]. Importantly, we now demonstrated that by integrating the pulmonary surfactant in the design of a core-shell drug delivery formulation, its beneficial effects on intracellular siRNA delivery are maintained. We noted a substantial decrease in cellular internalization for the hybrid nanoparticle, most likely attributed to the negative charge of the pulmonary surfactant outer layer, which reduces the interaction with the plasma membrane and therefore precludes efficient endocytic uptake. Remarkably, despite this observation, the coated siNGs-2 achieved the same gene silencing effect than their uncoated counterparts (**Figure 5**). Notably, assessing the intracellular fate of the nanoparticles *via* fluorescence colocalization analysis did not reveal any obvious differences in intracellular trafficking as both coated and uncoated formulations showed equal accumulation in LAMP-1 stained lysosomes (**Figure 7**). The elucidation of the exact mechanism *via* which the pulmonary surfactant promotes cytosolic siRNA delivery will likely require a more detailed investigation.
Given the substantial reduction in intracellular siRNA dose due to the presence of a protective outer layer, it can be postulated that the efficacy of our hybrid nanoparticle could be further enhanced by incorporating an active targeting ligand that drives receptor-mediated endocytosis. Folate has been widely used as targeting moiety for drug delivery in cancer therapy because of its high affinity and specificity for the folate receptor (FR), which is frequently overexpressed on the surface of a variety of human tumors [43, 44]. In this study, PEGylated lipids carrying a folate group at its distal end (DSPE-PEG_{2000}-folate) were incorporated in the pulmonary surfactant bilayer. The presence of PEG chains did not interfere with the deposition of a stable pulmonary surfactant shell, given that the inclusion of up to 10 wt% DSPE-PEG_{2000}-folate did not influence size or stability of the hybrid nanoparticles (**Figure S5**).
The presence of the folate targeting ligands clearly guided receptor-mediated cellular internalization in lung cancer cells. Moreover, we have identified that a critical surface density of folate is required to drive the receptor-mediated internalization process [45]. Most importantly, the increase in cellular siRNA dose linearly correlated with an improved RNAi effect, achieving a marked gene silencing in lung cancer cells at siRNA concentrations in the low nanomolar range. These results also indicate that altering the pulmonary surfactant composition by adding up to 10 wt% of PEGylated lipids does not debilitate its delivery-enhancing properties (**Figure 6**).

5. Conclusions

Taken together, we have developed a highly efficient, bio-inspired hybrid nanoparticle with promising features for siRNA inhalation therapy. The hybrid nanoparticle consists of a cationic biodegradable dextran nanogel core that is loaded with siRNA and is layered with a

pulmonary surfactant shell. We have found that the pulmonary surfactant shell improves the stability, potentiates intracellular siRNA delivery and enables the inclusion of targeting moieties. To date the instillation of exogenous pulmonary surfactant was solely used as standard therapeutic intervention for neonatal respiratory distress syndrome [46]. However, research is currently ongoing in order to understand how pulmonary surfactant replacement could benefit a wider range of lung diseases, since it was already indicated that pulmonary surfactant dysfunction contributes to the development and outcome of several respiratory diseases [47, 48]. This implies that our formulation, combining the high transfection efficiency of the dextran nanogels with the inherent therapeutic potential of a clinically approved pulmonary surfactant, provides new therapeutic opportunities for the treatment of lung diseases with underlying pulmonary surfactant dysfunction.

Acknowledgements
L. De Backer is a doctoral fellow of the Special Research Fund – Ghent University (BOF). K. Raemdonck is a postdoctoral fellow of the Research Foundation – Flanders, Belgium (FWO-Vlaanderen). Financial support of the Special Research Fund – Ghent University (BOF12/GOA/014) is also gratefully acknowledged.

Appendix A. Supplementary data
Supplementary data associated with this article can be found, in the online version, at doi:

References
[1] K. Raemdonck, R.E. Vandenbroucke, J. Demeester, N.N. Sanders, S.C. De Smedt, Maintaining the silence: reflections on long-term RNAi, Drug Discovery Today, 13 (2008) 917-931.
[2] B.L. Davidson, P.B. McCray, Current prospects for RNA interference-based therapies, Nat. Rev. Genet., 12 (2011) 329-340.
[3] R. Kole, A.R. Krainer, S. Altman, RNA therapeutics: beyond RNA interference and antisense oligonucleotides, Nat. Rev. Drug Discovery, 11 (2012) 125-140.
[4] P. Kubowicz, D. Zelaszczyk, E. Pekala, RNAi in clinical studies, Curr. Med. Chem., 20 (2013) 1801-1816.
[5] S.Y. Wu, G. Lopez-Berestein, G.A. Calin, A.K. Sood, RNAi therapies: drugging the undruggable, Sci. Transl. Med., 6 (2014) 240ps247.
[6] J. Wang, Z. Lu, M.G. Wientjes, J.L. Au, Delivery of siRNA therapeutics: barriers and carriers, AAPS J., 12 (2010) 492-503.
[7] R. Kanasty, J.R. Dorkin, A. Vegas, D. Anderson, Delivery materials for siRNA therapeutics, Nat. Mater., 12 (2013) 967-977.
[8] K. Singha, R. Namgung, W.J. Kim, Polymers in small-interfering RNA delivery, Nucleic Acid Ther., 21 (2011) 133-147.
[9] O.M. Merkel, T. Kissel, Quo vadis polyplex?, J. Controlled Release, 190 (2014) 415-423.
[10] S.C. Semple, A. Akinc, J. Chen, A.P. Sandhu, B.L. Mui, C.K. Cho, D.W. Sah, D. Stebbing, E.J. Crosley, E. Yaworski, I.M. Hafez, J.R. Dorkin, J. Qin, K. Lam, K.G. Rajeev, K.F. Wong, L.B. Jeffs, L. Nechev, M.L. Eisenhardt, M. Jayaraman, M. Kazem, M.A. Maier, M. Srinivasulu, M.J. Weinstein, Q. Chen, R. Alvarez, S.A. Barros, S. De, S.K. Klimuk, T. Borland, V. Kosovrasti, W.L. Cantley, Y.K. Tam, M. Manoharan, M.A. Ciufolini, M.A. Tracy, A. de Fougerolles, I. MacLachlan, P.R. Cullis, T.D. Madden, M.J. Hope, Rational design of cationic lipids for siRNA delivery, Nat. Biotechnol., 28 (2010) 172-176.
[11] S. Falsini, L. Ciani, S. Ristori, A. Fortunato, A. Arcangeli, Advances in lipid-based platforms for RNAi therapeutics, J. Med. Chem., 57 (2014) 1138-1146.
[12] Q. Lin, J. Chen, Z. Zhang, G. Zheng, Lipid-based nanoparticles in the systemic delivery of siRNA, Nanomedicine (London, U.K.), 9 (2014) 105-120.
[13] K. Raemdonck, B. Naeye, K. Buyens, R.E. Vandenbroucke, A. Hogset, J. Demeester, S.C. De Smedt, Biodegradable Dextran Nanogels for RNA Interference: Focusing on Endosomal Escape and Intracellular siRNA Delivery, Adv. Funct. Mater., 19 (2009) 1406-1415.
[14] K. Raemdonck, K. Braeckmans, J. Demeester, S.C. De Smedt, Merging the best of both worlds: hybrid lipid-enveloped matrix nanocomposites in drug delivery, Chem. Soc. Rev., 43 (2014) 444-472.
[15] B. Mandal, H. Bhattacharjee, N. Mittal, H. Sah, P. Balabathula, L.A. Thoma, G.C. Wood, Core-shell-type lipid-polymer hybrid nanoparticles as a drug delivery platform, Nanomedicine (N.Y., NY, U.S.), 9 (2013) 474-491.

[16] K. Hadinoto, A. Sundaresan, W.S. Cheow, Lipid-polymer hybrid nanoparticles as a new generation therapeutic delivery platform: a review, Eur. J. Pharm. Biopharm., 85 (2013) 427-443.
[17] X.Z. Yang, S. Dou, Y.C. Wang, H.Y. Long, M.H. Xiong, C.Q. Mao, Y.D. Yao, J. Wang, Single-step assembly of cationic lipid-polymer hybrid nanoparticles for systemic delivery of siRNA, ACS Nano, 6 (2012) 4955-4965.
[18] D. Peer, E.J. Park, Y. Morishita, C.V. Carman, M. Shimaoka, Systemic leukocyte-directed siRNA delivery revealing cyclin D1 as an anti-inflammatory target, Science, 319 (2008) 627-630.
[19] A. de Fougerolles, T. Novobrantseva, siRNA and the lung: research tool or therapeutic drug?, Curr. Opin. Pharmacol., 8 (2008) 280-285.
[20] C. Chang, Unmet Needs in Respiratory Diseases, Clin. Rev. Allergy Immunol., 45 (2013) 303-313.
[21] O.M. Merkel, I. Rubinstein, T. Kissel, siRNA delivery to the lung: what's new?, Adv. Drug Delivery Rev., 75 (2014) 112-128.
[22] S.C. Balmert, S.R. Little, Biomimetic delivery with micro- and nanoparticles, Adv. Mater. (Weinheim, Ger.), 24 (2012) 3757-3778.
[23] J.W. Yoo, D.J. Irvine, D.E. Discher, S. Mitragotri, Bio-inspired, bioengineered and biomimetic drug delivery carriers, Nat. Rev. Drug Discovery, 10 (2011) 521-535.
[24] J.J. Haitsma, U. Lachmann, B. Lachmann, Exogenous surfactant as a drug delivery agent, Adv. Drug Delivery Rev., 47 (2001) 197-207.
[25] W. Bernhard, C.J. Pynn, Therapeutic Lung Surfactants as Carriers for other Therapeutics-a Matter of Vision, Courage and Determination, Pediatr. Pulmonol., 44 (2009) 1157-1158.
[26] A.H. Jobe, T. Ueda, J.A. Whitsett, B.C. Trapnell, M. Ikegami, Surfactant enhances adenovirus-mediated gene expression in rabbit lungs, Gene Ther., 3 (1996) 775-779.
[27] J.P. Katkin, R.C. Husser, C. Langston, S.E. Welty, Exogenous surfactant enhances the delivery of recombinant adenoviral vectors to the lung, Hum. Gene Ther., 8 (1997) 171-176.
[28] J. Nguyen, R. Reul, T. Betz, E. Dayyoub, T. Schmehl, T. Gessler, U. Bakowsky, W. Seeger, T. Kissel, Nanocomposites of lung surfactant and biodegradable cationic nanoparticles improve transfection efficiency to lung cells, J. Controlled Release, 140 (2009) 47-54.
[29] L. De Backer, K. Braeckmans, J. Demeester, S.C. De Smedt, K. Raemdonck, The influence of natural pulmonary surfactant on the efficacy of siRNA-loaded dextran nanogels, Nanomedicine (London, U.K.), 8 (2013) 1625-1638.
[30] W.N.E. vanDijkWolthuis, S.K.Y. Tsang, J.J. KettenesvandenBosch, W.E. Hennink, A new class of polymerizable dextrans with hydrolyzable groups: hydroxyethyl methacrylated dextran with and without oligolactate spacer, Polymer, 38 (1997) 6235-6242.
[31] O. Blanco, J. Perez-Gil, Biochemical and pharmacological differences between preparations of exogenous natural surfactant used to treat Respiratory Distress Syndrome: Role of the different components in an efficient pulmonary surfactant, Eur. J. Pharmacol., 568 (2007) 1-15.
[32] H. Zhang, Q. Fan, Y.E. Wang, C.R. Neal, Y.Y. Zuo, Comparative study of clinical pulmonary surfactants using atomic force microscopy, Biochim. Biophys. Acta, 1808 (2011) 1832-1842.
[33] K. Braeckmans, K. Buyens, W. Bouquet, C. Vervaet, P. Joye, F. De Vos, L. Plawinski, L. Doeuvre, E. Angles-Cano, N.N. Sanders, J. Demeester, S.C. De Smedt, Sizing Nanomatter in Biological Fluids by Fluorescence Single Particle Tracking, Nano Lett., 10 (2010) 4435-4442.
[34] K. Braeckmans, D. Vercauteren, J. Demeester, S.C. De Smedt, Single particle tracking, Taylor and Francis, NY, USA., 2010.
[35] B. Naeye, H. Deschout, M. Roding, M. Rudemo, J. Delanghe, K. Devreese, J. Demeester, K. Braeckmans, S.C. De Smedt, K. Raemdonck, Hemocompatibility of siRNA loaded dextran nanogels, Biomaterials, 32 (2011) 9120-9127.
[36] G.R. Dakwar, E. Zagato, J. Delanghe, S. Hobel, A. Aigner, H. Denys, K. Braeckmans, W. Ceelen, F.C. De Smedt, K. Remaut, Colloidal stability of nano-sized particles in the peritoneal fluid: Towards optimizing drug delivery systems for intraperitoneal therapy, Acta Biomater., 10 (2014) 2965-2975.
[37] K. Buyens, B. Lucas, K. Raemdonck, K. Braeckmans, J. Vercammen, J. Hendrix, Y. Engelborghs, S.C. De Smedt, N.N. Sanders, A fast and sensitive method for measuring the integrity of siRNA-carrier complexes in full human serum, J. Controlled Release, 126 (2008) 67-76.
[38] J. Kuntsche, J.C. Horst, H. Bunjes, Cryogenic transmission electron microscopy (cryo-TEM) for studying the morphology of colloidal drug delivery systems, Int. J. Pharm., 417 (2011) 120-137.
[39] O.M. Merkel, A. Beyerle, D. Librizzi, A. Pfestroff, T.M. Behr, B. Sproat, P.J. Barth, T. Kissel, Nonviral siRNA Delivery to the Lung: Investigation of PEG-PEI Polyplexes and Their In Vivo Performance, Mol. Pharm., 6 (2009) 1246-1260.
[40] K.J. Tierney, D.E. Block, M.L. Longo, Elasticity and phase behavior of DPPC membrane modulated by cholesterol, ergosterol, and ethanol, Biophys. J., 89 (2005) 2481-2493.

[41] D.J. Giard, S.A. Aaronson, G.J. Todaro, P. Arnstein, J.H. Kersey, H. Dosik, W.P. Parks, In-Vitro Cultivation of Human Tumors - Establishment of Cell Lines Derived from a Series of Solid Tumors, J. Natl. Cancer Inst., 51 (1973) 1417-1423.
[42] C.E. Ashley, E.C. Carnes, K.E. Epler, D.P. Padilla, G.K. Phillips, R.E. Castillo, D.C. Wilkinson, B.S. Wilkinson, C.A. Burgard, R.M. Kalinich, J.L. Townson, B. Chackerian, C.L. Willman, D.S. Peabody, W. Wharton, C.J. Brinker, Delivery of small interfering RNA by peptide-targeted mesoporous silica nanoparticle-supported lipid bilayers, ACS Nano, 6 (2012) 2174-2188.
[43] W. Xia, P.S. Low, Folate-Targeted Therapies for Cancer, J. Med. Chem., 53 (2010) 6811-6824.
[44] N. Kamaly, Z.Y. Xiao, P.M. Valencia, A.F. Radovic-Moreno, O.C. Farokhzad, Targeted polymeric therapeutic nanoparticles: design, development and clinical translation, Chem. Soc. Rev., 41 (2012) 2971-3010.
[45] F. Gu, L. Zhang, B.A. Teply, N. Mann, A. Wang, A.F. Radovic-Moreno, R. Langer, O.C. Farokhzad, Precise engineering of targeted nanoparticles by using self-assembled biointegrated block copolymers, Proc. Natl. Acad. Sci. U.S.A., 105 (2008) 2586-2591.
[46] W.A. Engle, F. American Academy of Pediatrics Committee on, Newborn, Surfactant-replacement therapy for respiratory distress in the preterm and term neonate, Pediatrics, 121 (2008) 419-432.
[47] J.A. Whitsett, S.E. Wert, T.E. Weaver, Alveolar surfactant homeostasis and the pathogenesis of pulmonary disease, Annu. Rev. Med., 61 (2010) 105-119.
[48] E. Lopez-Rodriguez, J. Perez-Gil, Structure-function relationships in pulmonary surfactant membranes: from biophysics to therapy, Biochim. Biophys. Acta, 1838 (2014) 1568-1585.